The Chemistry of Adsorbed Cu(II) and Mn(II) in Aqueous Titanium Dioxide Suspensions

WILLIAM F. BLEAM* AND MURRAY B. MCBRIDE†

*Departments of *Chemistry and †Agronomy Cornell University, Ithaca, New York*

We studied the adsorption behavior of Cu(II) and Mn(II) on the surface of titanium dioxide over the pH range from 2.0 to 11.5. The titanium dioxide we used in these experiments was prepared by hydrolyzing $TiCl_4$ and had a surface area of 113.7 $m^2\ g^{-1}$. All suspensions, which were 9.04×10^{-3} *M* in $NaClO_4$, contained 20 m^2 $liter^{-1}$ of oxide surface and divalent metal ion concentrations sufficient (at full adsorption from solution) to cover the available surface with one-half, one, and four layers of close-packed, hydrated ions. Both divalent ions began adsorption below titanium dioxide's isoelectric point (pH = 6.2). Cu^{2+} adsorption was accompanied by net OH^- uptake from solution and it was inferred that the titania surface also provided OH^- for Cu^{2+} adsorption. ESR spectra demonstrate the coexistence of two distinct forms adopted by these metal ions on the surface. A portion of the adsorbed metal ions occupies sites magnetically isolated one from another, as evidenced by the paramagnetic behavior of this form. The majority of the metal ions, however, exist in hydrous-metal–ion clusters in which spin-exchange coupling of the electron dipoles determines the magnetic behavior. Electrophoretic mobility measurements indicate that ions adsorbed at isolated sites exert a stronger influence on the electrophoretically measured charge of the suspension particles than ions in clusters. Even though these experiments were performed in the absence of oxygen, we observed the oxidation of a limited amount of the Mn(II) on the surface as low as pH = 5. Presumably this occurs as a result of electron transfer between photo-induced electron holes and Mn(II) on the surface.

INTRODUCTION

The study of transition metal ions adsorbed on oxide surfaces has proceeded as two rather distinct efforts. The first is concerned with the equilibrium between aqueous metal-ion solutions and the oxide adsorbent, where the detailed properties of the solution are carefully related to processes occurring on the oxide surface. The second has as its major interest the catalytic properties of metal ions supported on various oxides.

Workers involved in the former effort have shown that in certain cases metal ions can adsorb from aqueous solution at localized oxide surface sites where a "coordination complex" forms. Surface complexation constants for such "coordination complexes" have been determined using a variety of models (1–3). Recently, some authors have estimated surface complexation constants based on the correlation existing between electron spin resonance (ESR) parameters and stability constants for coordination complexes formed in solution (4–6). This correlation is based on the relation between these parameters and the coordination environment of the metal ion in the complex (6–9).

The catalytic literature regarding transition metal ions on oxide surfaces often focuses on catalysts prepared at high temperatures. While metal ions adsorbed at localized sites have received much attention, surface clusters have also been recognized as a common form adopted by adsorbed ions. The motivating observation has been the discrepancy between magnetic susceptibility and ESR measurements. That is, while all of the transition metal dispersed on a surface contribute to the magnetic susceptibility, often only a small fraction

contributes to the observed ESR signal (10–16).

The conclusion often reached has been that the distribution of metal ions on the surface is not uniform, even at the lowest concentrations on the surface (10, 12, 16–19). The ESR spectra have been interpreted as composite spectra arising from both metal ions adsorbed at magnetically isolated sites (paramagnets) and in surface clusters (ferri-, ferro-, or antiferromagnets). The adsorbents used in these studies included zeolites (13, 20), silica (14), alumina (10–12, 16, 17, 19) and amorphous aluminosilicates (18). Our objective in the research reported herein was to see whether and under what conditions surface clusters formed when Cu(II) and Mn(II) were allowed to equilibrate with aqueous titanium dioxide suspensions.

MATERIALS

We synthesized titanium dioxide by adding titanium tetrachloride to distilled, deionized water (H_2O:$TiCl_4$ = 2:1) and refluxing the hydrolyzed suspension for 4 h. The oxide was washed repeatedly with distilled, deionized water until the suspension was free of chloride, then freeze-dried. We measured the specific surface area by the BET method with N_2 as the adsorbing gas. The surface area was 113.7 $m^2\ g^{-1}$.

METHODS

The methods we used in this study are detailed elsewhere (16). The surface area in all suspensions was 20 m^2 $liter^{-1}$. All experiments were conducted under a nitrogen atmosphere in oxygen-free solutions containing 9.04×10^{-3} *M* $NaClO_4$ as the background electrolyte to maintain a constant ionic strength. Taking the hydrated radius of the divalent ions to be 3.42×10^{-10} *m*, complete adsorption of 9.04×10^{-5} *M* Cu(II) or Mn(II) by an oxide suspension with 20 m^2 $liter^{-1}$ surface area would, at most, cover the surface with a close-packed monolayer of hydrated ions. We use this concentration, or multiples of it, as a means of relating the amount adsorbed to the *potential* coverage of the surface. We do not imply that once the ions are adsorbed they necessarily cover the surface as close-packed, hydrated ions.

RESULTS

I. Titanium Dioxide Suspensions Containing Cu(II)

The electrophoretic mobility (EM) of titanium dioxide suspensions over a range of pH and containing various amounts of Cu(II) are shown in Fig. 1. The pH of zero particle mobility in Cu(II)-free suspensions, which we refer to as the isoelectric point (IEP), is 6.2. The ionic strength of the solutions and the particle size of the titanium dioxide satisfy the Helmholtz–Smoluchowski limiting conditions (21). The ζ potential at pH = 2.0, determined using the Helmholtz–Smoluchowski formula, is 54 mV.

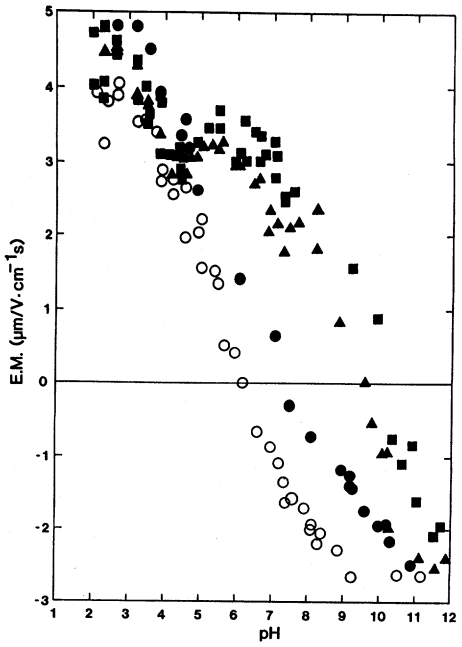

FIG. 1. The variation of the electrophoretic mobility of suspension particles as a function of pH for titanium dioxide suspensions (20 m^2 $liter^{-1}$) in 9.04×10^{-3} *M* $NaClO_4$ (○) and three initial concentrations of $Cu(NO_3)_2$: (●) 4.52×10^{-5}, (▲) 9.04×10^{-5}, and (■) 3.61×10^{-4} *M*.

Figure 2 shows the surface excess concentration of Cu(II), Γ_{Cu}, as a function of pH. The initial concentrations (4.52×10^{-5}, 9.04×10^{-5} and 3.61×10^{-4} *M*) correspond to sufficient Cu(II) in solution to cover the surface (upon complete adsorption from solution) with one-half, one, and four layers of close-packed, hydrated ions. Adsorption of Cu(II) begins in the pH range 2.0–2.3, well below the IEP of the titanium dioxide. At pH = 4.4 there is an abrupt increase in the surface excess concentration of Cu(II).

Cu(II) adsorption altered the hydroxyl sorption properties of the suspension in the pH range 3.7–5.1. Outside this range the pH dependent hydroxyl sorption by the suspension was not measurably affected by the presence of Cu(II). In Cu-free TiO_2 suspensions the transition from net hydroxyl desorption to net adsorption occurs at pH = 5.1, while the same suspensions with Cu(II) present have this transition at pH = 3.7. Thus, the adsorption Cu(II) leads to enhanced hydroxyl adsorption (or proton release) by the surface.

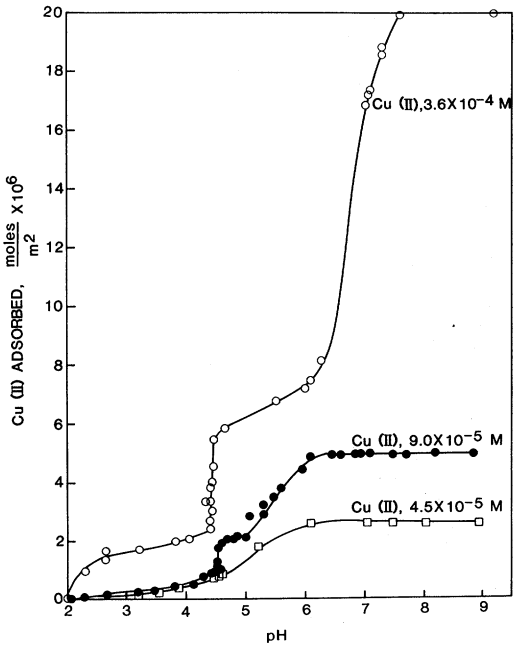

FIG. 2. The variation of the surface excess concentration of Cu(II) adsorbed as a function of pH for titanium dioxide suspensions (20 m^2 $liter^{-1}$) in 9.04×10^{-3} *M* $NaClO_4$ and three initial concentrations of $Cu(NO_3)_2$: 4.52×10^{-5}, 9.04×10^{-5}, and 3.61×10^{-4} *M*.

We calculated the surface excess concentration of hydroxyl, Γ_{OH}, in the pH range 3.8 to 5.1. The ratio, Γ_{OH}/Γ_{Cu}, increases with pH, reaching it maximum value in the pH range 4.4–4.6, then decreases with pH. In fact, the maximum in Γ_{OH}/Γ_{Cu} occurred at pH = 4.6, 4.5, and 4.4 for the low, medium, and high levels of added Cu(II), respectively, the same pHs at which the surface excess concentration of Cu(II) increased abruptly in those systems. The maximum values of Γ_{OH}/Γ_{Cu} were in the range of 1.5–1.8, with the lower levels of Cu(II) adsorption having the higher Γ_{OH}/Γ_{Cu} ratios.

Since TiO_2 desorbs hydroxyls below pH = 5.1 and adsorbs hydroxyls above this pH, the TiO_2 surface can be considered a sink for protons below and a source above that pH. In a similar sense the solution can also be considered a source and sink for protons. As the pH of the suspension increases toward pH = 5.1 the TiO_2 surface has a decreasing affinity for protons, and as such becomes a less favorable sink for protons, while the solution becomes a more favorable sink because of the increased activity of hydroxyls at higher pHs.

When Cu(II) adsorbs hydrolysis occurs and the protons released can enter either of these sinks. Given the hydroxyl desorption properties of the TiO_2 surface, we would expect the Γ_{OH}/Γ_{Cu} ratios to increase with pH, which does occur up to pH = 4.4–4.6. Furthermore, the lower Γ_{OH}/Γ_{Cu} values at higher Cu(II) addition levels may result from the lower hydroxyl to Cu(II) activity ratios in the more concentrated Cu(II) solutions at a given pH. Thus, Cu(II) adsorption in suspensions containing a higher solution concentration of Cu(II) is more likely to release protons to the TiO_2 surface than the solution.

In the pH range 4.4 to 4.6, where the Γ_{OH}/Γ_{Cu} ratios reach their maximum, an important transition occurs. As we mentioned above, the pH at which the Γ_{OH}/Γ_{Cu} ratio reaches its maximum in a given suspension is also the pH at which the surface excess concentration

of Cu(II) abruptly increases. Above this pH the ratios decrease as pH increases. We are unable to explain why this occurs.

Adsorption of all Cu(II) in solution is complete by pH = 6.1 for the two lowest levels of Cu(II) used in our experiments. The solubility product of cupric hydroxide is exceeded at pH = 6.2 in the system with the highest Cu(II) concentration. We have plotted the data in Fig. 2 as the surface excess concentration of Cu(II) although for the highest Cu(II) level this strictly applies for pH values less than 6.2. At the two lowest Cu(II) levels, adsorption is complete at a pH below the onset of $Cu(OH)_2(s)$ precipitation.

We have plotted pCu versus pH for the adsorption experiments in Fig. 3. The decrease in Cu(II) above pH = 4.5 appears to differ between the suspensions with the two lowest Cu(II) concentrations and the highest concentration. In the former cases, pCu and pH change in such a manner that the data points curve away from the cupric hydroxide solubility line as it is approached. In the latter case, the data points trend, with little or no curvature, toward the hydroxide solubility line until precipitation occurs at pH = 6.2.

Clearly, the effect on EM by Cu(II) adsorption is not directly proportional to the quantity adsorbed (Compare Figs. 1 and 2). Much of

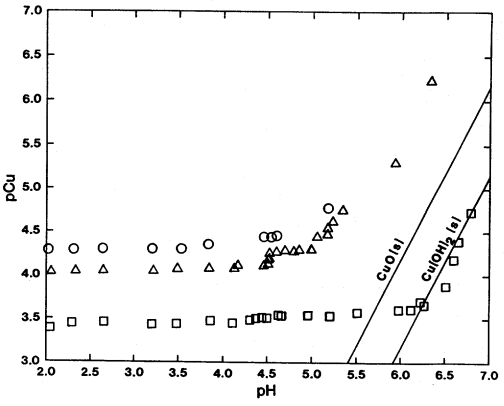

FIG. 3. Diagram showing the variation of pCu as a function of pH for the titanium dioxide suspensions of Fig. 2. (○) Cu(II), 4.52×10^{-5} *M*; (△) Cu(II), 9.04×10^{-5} *M*; (□) Cu(II), 3.61×10^{-4} *M*.

the increase in particle EM has occurred by the point where full adsorption of the intermediate Cu(II) level (sufficient to form a full monolayer of close-packed, hydrated ions) is complete. The pH at which the deviation in EM of Cu(II)-containing relative to Cu(II)-free suspensions arises is the same pH at which the sharp increase in the surface excess concentration of Cu(II) occurs.

A selection of typical ESR spectra taken from titanium dioxide suspensions containing sufficient Cu(II) to form a full monolayer are shown in Fig. 4. The ESR spectrum at pH = 2.7 (Fig. 4A) is typical of Cu(II) in "static," tetragonally-distorted octahedral coordination. By "static" we mean the orientation of the elongated symmetry axis does not change on the time scale of the ESR measurement. This signal grows in intensity as the pH increases to 3.2 (Fig. 4B) while showing signs of broadening. Broadening has nearly obscured the signal by pH = 3.5 (Fig. 4C).

The ESR spectrum changes drastically at pH = 4.4, the spectrum appearing in Fig. 4D being typical of those arising at pH = 4.4. We clearly see the spectrum for paramagnetic Cu(II) in "static" tetragonal coordination superimposed on an intense symmetric signal. The parallel component of the g value for tetragonal Cu(II) has changed from $g = 2.328$ at pH = 2.7 to $g = 2.356$ at pH = 4.5 indicating the crystal field is stronger in the former case. This type of spectrum persists until pH = 5.6 with a gradual increase in broadness.

By pH = 5.9 (Fig. 4E) this signal has broadened considerably and continues to broaden (Fig. 4F) and lose intensity up to about pH = 9, after which the signal is almost lost. At pH = 11.1 (Fig. 4G) the spectrum due to Cu(II) in "static" tetragonal coordination reappears, superimposed on a much broadened symmetric signal, and persists to the highest pHs included in this study (Fig. 4H). Note that $g = 2.349$ (Fig. 4H) is not substantially different from the value of g at pH = 4.5 (Fig. 4D).

This same series of ESR spectra just described is observed for systems containing the lowest Cu(II) level and the highest Cu(II) level

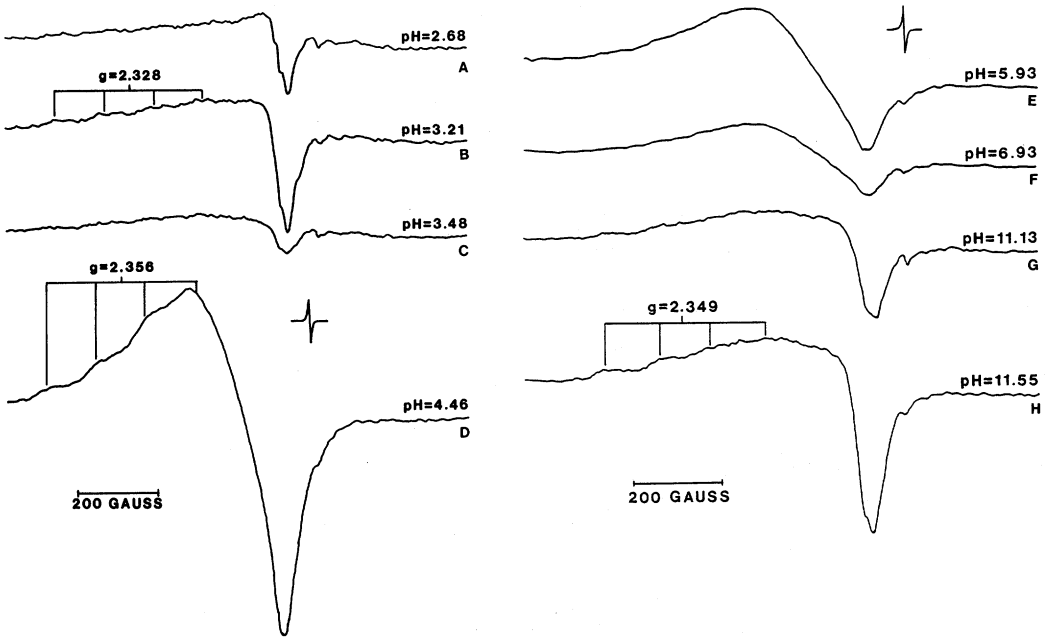

FIG. 4. Electron-spin resonance spectra for Cu(II) in selected titanium dioxide suspensions. Initial concentration of $Cu(NO_3)_2$ was 9.04×10^{-5} *M*.

with certain important exceptions. Beginning with the spectra observed for systems with the lowest Cu(II) level, the spectrum similar to Fig. 4D is less intense. The high pH signal for Cu(II) in "static" tetragonal coordination reappears at pH = 9.9 compared to pH = 11.1 in suspensions containing the intermediate Cu(II) level. Because the symmetric peak upon which it is superimposed continues to broaden as the pH increases above pH = 9.9, the "static" tetragonal Cu(II) signal becomes increasingly well defined at higher pH.

There are three important exceptions to the pattern of ESR spectra for the highest Cu(II) level relative to those appearing in Fig. 4. First, the appearance of spectra similar to the one in Fig. 4D occurs at a significantly lower pH, 4.1 vs 4.4. Second, the ESR spectrum has broadened to the point where it is barely visible by pH = 6.0. Finally, a spectrum for paramagnetic Cu(II) in "static" tetragonal coordination never reappears at high pH as was the case for the lowest two Cu(II) levels.

In summary, Cu(II) adsorption begins below the IEP of titanium dioxide at about pH = 2.0–2.3 and the surface excess concentration rises sharply in the pH range of 4.4–4.6. Adsorption is more gradual at pHs above 4.6 and, at the two lowest Cu(II) levels, is complete by pH = 6.1. Precipitation of cupric hydroxide occurs at pH = 6.2 in the systems with an initial Cu(II) concentration of 3.61×10^{-4} *M*. A significant increase in the magnitude of suspension particle electrophoretic charge for Cu(II)-containing suspensions arises at about pH = 4.5, expressed as a higher EM at a given pH relative to Cu(II)-free suspensions. The ESR data indicate a broadening of the spectra of *paramagnetic* Cu(II) in "static" tetragonal coordination at pH = 3.5 and the appearance of a broad, symmetric signal without hyperfine structure upon which a "static" tetragonal signal is superimposed at about pH = 4.4 when surface coverage is still quite low. Furthermore, paramagnetic Cu(II) ions adsorbed on the surface exist at high pH when the amount of Cu(II) adsorbed is sufficient to form a monolayer of close-packed, hydrated ions.

II. Titanium Dioxide Suspensions Containing Mn(II)

The surface excess concentration of Mn(II) as a function of pH in aqueous titanium dioxide suspensions is shown in Fig. 5. The Mn(II) levels we used correspond to sufficient Mn(II) to cover the surface, upon complete adsorption from solution, with either one or four complete monolayers of close-packed, hydrated ions. Adsorption of Mn(II) on titanium dioxide appears to begin in the pH range of 2–3 with a relatively small amount of Mn(II) adsorbed at pH values below the oxide's IEP. Beginning at pH = 5 adsorption is accompanied by the rapid oxidation of a *limited* amount of Mn(II) even though these experiments were performed in the absence of oxygen. The extent of this oxidation did not appear to increase as the pH increased above 5.

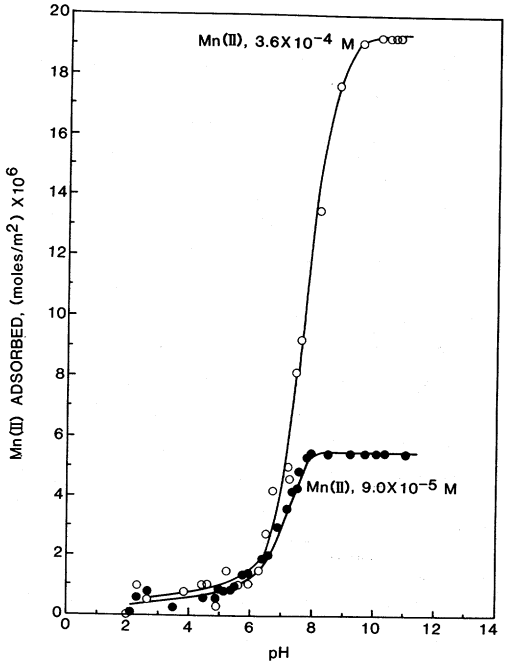

FIG. 5. The variation of the surface excess concentrations of Mn(II) adsorbed as a function of pH for titanium dioxide suspensions (20 m^2 $liter^{-1}$) in 9.04×10^{-3} M $NaClO_4$ and two initial concentrations of $Mn(ClO_4)_2$: 9.04×10^{-5} and 3.61×10^{-4} M.

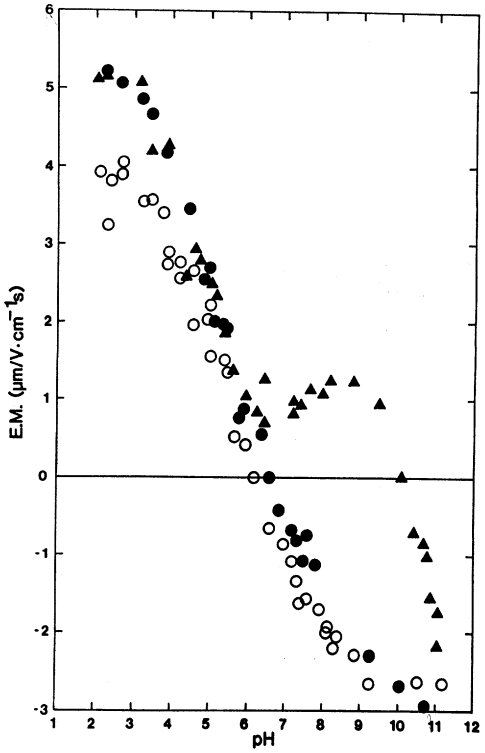

FIG. 6. The variation of the electrophoretic mobility of suspension particles as a function of pH for titanium dioxide suspensions (20 m^2 $liter^{-1}$) in 9.04×10^{-3} M $NaClO_4$ and two initial concentrations of $Mn(ClO_4)_2$: (●) 9.04×10^{-5} and (▲) 3.61×10^{-4} M.

The solubility product of manganous hydroxide was never exceeded in these experiments. Full adsorption from solution was complete by pH = 7.8 for those systems containing 9.04×10^{-5} M Mn(II) and pH = 9.5 for those containing 3.61×10^{-4} M Mn(II). The equilibrium constant for the first hydrolysis of hexaquomanganese(2+) is $pK_1 = 11.07$. Even at pH = 9.5 only 3% of the Mn(II) remaining in solution is hydrolyzed.

The effect of Mn(II) adsorption on the EM of suspension particles (Fig. 6) differs from what we observed for Cu(II). Adsorption of sufficient Mn(II) to *potentially* cover the titanium dioxide surface with a monolayer of close-packed, hydrated ions has no apparent effect on the EM of the particles. On the other hand, we observe an increase in the EM at pH

= 6.5 for systems containing the highest Mn(II) level, ultimately increasing the pH of zero particle mobility to pH = 10.

In systems containing Cu(II), adsorption of the "equivalent" of a monolayer results in an increase in EM nearly as great as when the "equivalent" of four monolayers of Cu(II) have adsorbed. Systems containing Mn(II) show no noticeable increase in EM after the adsorption of the "equivalent" of a monolayer. However, full adsorption from solutions containing the highest Mn(II) level increase the pH of zero particle mobility to nearly the same value as when an equal amount of Cu(II) is adsorbed.

The solution concentrations of Cu(II) used in these experiments were below the detection limits of the ESR spectrometer we used. As a result, any Cu(II) spectrum can be attributed to species on the surface because the adsorption process increases the amount of Cu(II) in the sample volume to the point where Cu(II) is detectable by our spectrometer. The concentrations of Mn(II) in solution are much higher than our instrument's detected detection limits for Mn(II) and solution species give a very strong signal. As a result, signals due to Mn(II) on the surface are masked by the signal from solution species so long as significant amounts of Mn(II) remain in solution.

For those systems containing the lower level of Mn(II), an ESR spectrum due to Mn(II) on the surface is first evident at pH = 5.5. The general characteristics of this spectrum remain unchanged up to pH = 7.6 (Figs. 7A and 7B). The six hyperfine peaks characteristic of paramagnetic Mn(II) in octahedral coordination are clearly apparent; however, these peaks are much broader than those in the spectrum of hexaquomanganese(2+) in solution. These hyperfine peaks appear to be superimposed on a much broader peak (ΔH = 500 G).

The solution spectrum masks the spectrum from surface species until pH = 8.8 in those systems with the highest level of Mn(II). At this point (Fig. 7C) the spectrum consists of six, broadened hyperfine peaks superimposed upon a very broad, weak signal. This latter

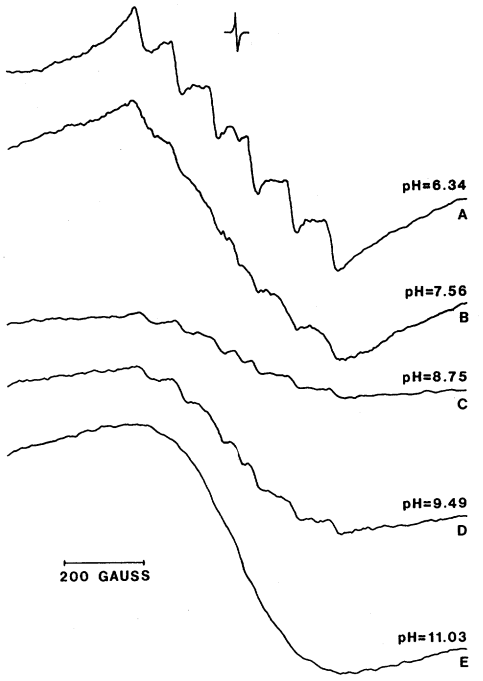

FIG. 7. Electron-spin resonance spectra for manganese(II) in selected titanium dioxide suspensions.

broad signal (ΔH = 500 G) grows in intensity as the pH increases to 11 (Figs. 7D and E).

The temperature dependence of the spectrum of Fig. 7A appears in Fig. 8. The hyperfine peaks become narrower as the temperature is lowered and reach a minimum at 173 K. If we measure the intensity from the half height of the first hyperfine peak to the half height of the last hyperfine peak (I in Fig. 8) and plot the inverse of this intensity versus the temperature the relation is linear with a positive intercept. This is characteristic behavior of an antiferromagnet [cf. (16)]. A plot of the inverse peak intensity for spectra shown in Figs. 7D and E is also indicative of antiferromagnets.

To summarize, adsorption of Mn(II) on titanium dioxide begins in the pH range of 2 to 3. At and above pH = 5 a limited amount of the Mn(II) in the system oxidizes on the surface, turning the suspension light brown. The extent of oxidation does not appear to increase significantly with pH. The adsorbed Mn(II)

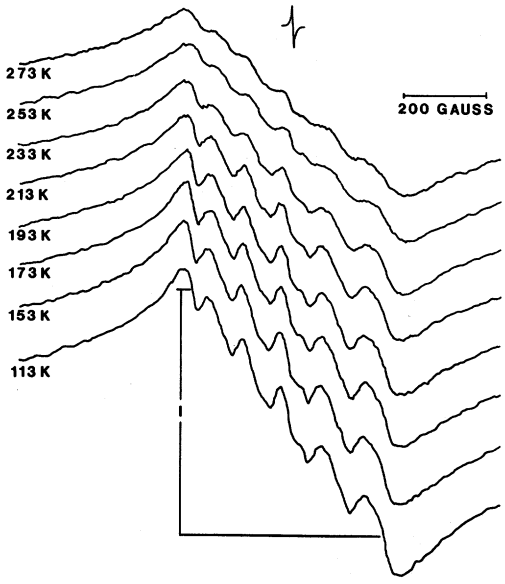

FIG. 8. The temperature dependence of the electron spin resonance spectrum shown in Fig. 7A. The gain setting was half that used in recording the spectrum in Fig. 7A.

does not disperse uniformly over the surface. Even when the amount adsorbed is sufficient to cover the surface with nearly four layers of close-packed ions the ESR data indicate the presence of both magnetically isolated and strongly coupled species on the surface (cf. Figs. 7C and D).

DISCUSSION

The ESR spectrum of Cu(II) observed at pH = 2.7 (Fig. 4A) is characteristic of Cu(II) in tetragonal coordination, a distorted octahedral environment with axial symmetry in which the symmetry axis is elongated (22). Implicit in this analysis is the recognition that the system of Cu(II) ions giving rise to such a spectrum exist as paramagnets. Furthermore, the orientation of the symmetry axis of Cu(II) in this coordination environment must be "static" on the time scale of the ESR measurement. Such a spectrum can be attributed to Cu(II) chemisorbed at magnetically isolated sites on the titanium oxide surface. In the limit of very high dispersion on a surface (22) the hyperfine peaks of both the parallel and perpendicular components of the anisotropic g tensor are apparent in the spectrum.

Broadening of the spectrum for Cu(II) adsorbed on oxide surfaces and on ion exchange resins is commonly observed as the concentration of Cu(II) ions on the absorbent increases. This broadening is the result of the interaction of magnetic dipoles both through the classical mechanism of dipole–dipole coupling or through the quantum mechanical phenomenon of spin-exchange coupling. It is generally accepted that spin-exchange coupling dominates systems of electron dipoles (24–26).

In many systems, with absorbents ranging from polymeric ion exchangers and zeolites to oxide surfaces, spectra similar to the ones we observed (Figs. 4D and E) have been reported by other workers (10–13, 17, 20, 23, 27–33). Some are interpreted as resulting from exchange-broadened paramagnetic Cu(II) (27, 28, 32). Others attribute such a spectrum to salt crystals which form when the solution is frozen (29, 30, 33). McBride (17) observed a spectrum similar to Fig. 4F for Cu(II) adsorbed on gibbsite and attributed this to cupric hydroxide precipitated on the surface. There seems to be no question that it is the result of magnetically coupled ions.

It is important to recognize that the *absence* of an ESR signal does not constitute proof that certain species do not exist. As pointed out by Berger and Roth (12), ESR measures magnetically isolated ions and coupled ions in small domains. Magnetic susceptibility measurements integrate over a broad spectrum of domains ranging from magnetically isolated ions to bulk solids such as cupric oxide. While it is true that relaxation processes in bulk, magnetically ordered materials often render the ESR signal extremely broad, it is possible to observe the ferromagnetic resonance spectrum arising from small domains (16).

Initial adsorption of Cu(II) begins at sites with a relatively high crystal field strength. The Cu(II) ions first adsorbed are clearly isolated, but the ESR spectra from adsorbed Cu(II) has

broadened considerably by pH = 3.5 (Fig. 4C). If the ions adsorbed by pH = 3.5, in the case of Fig. 4C, were uniformly distributed the mean separation would be 2.3×10^{-9} m. If we attribute the broadening we observe at pH = 3.5 to spin-exchange and recognize that ions separated by 2.3×10^{-9} *m* would be magnetically isolated, then it follows that the sites first occupied are not uniformly distributed on the surface. The sites occupied by Cu(II) at pH = 2.7 (whose ESR spectra are broadened by pH = 3.5) may be close enough together that, as they are populated, exchange coupling arises while the average surface coverage is still quite low.

The analysis by several authors (19, 29, 31, 33) clearly demonstrates the composite nature of the type of spectrum shown in Fig. 4D, consisting of a symmetric signal superimposed on the parallel and perpendicular components of paramagnetic Cu(II) in "static" tetragonal coordination. Martini *et al.* (29) and Fujiwara *et al.* (33) ascribe the symmetric peak at $g = 2.16$ to Cu(II) salts formed when Cu(II)-containing solutions were frozen. Cozar and Znamirovaschi (31) and Cozar *et al.* (19) assign the same symmetric peak to clusters of Cu(II) on the surface. Hornsky and Rakos (23) specifically rule out cluster formation and attribute a similar spectrum [Fig. 1a of their paper] to Cu(II) uniformly distributed on the surface, broadened by exchange coupling. We consider Fig. 4D a composite spectrum due to paramagnetic Cu(II) in tetragonal coordination and exchange coupled Cu(II) in surface clusters. At pH = 4.4 these clusters have nucleated and begin a stage of rapid growth over the rather narrow pH range from 4.4 to 4.6.

The interval in which cluster formation occurs is also characterized by the appearance of Cu(II) occupying sites with a weaker crystal field than those occupied at pH = 2.6, as evidenced by the difference in *g* values. Isolated sites still exist in suspensions containing sufficient Cu(II) to form a complete monolayer as demonstrated by the appearance of a paramagnetic signal at pH = 11. (Note: Reorganization of Cu(II) on the surface may have occurred leading to the reappearance of a paramagnetic signal at pH = 11.) Apparently magnetically isolated sites no longer exist in suspensions containing the highest level of Cu(II) used in these experiments. Whether or not the solubility product for bulk cupric hydroxide is exceeded is probably determined by the size of surface clusters formed. It is likely that a mass action balance controls growth of surface clusters relative to the adsorption of isolated sites.

The effect of adsorption on EM is more difficult to explain. While EM does not measure the true ZPC (34), it does reflect the charge arising from the "clean" surface, isolated adsorbates and surface clusters. Clearly, several factors are important in determining the final net electrophoretically measured charge. There are both extensive factors (e.g., the total area of "clean" surface, total area of surface clusters and total numbers of isolated ions) and intensive factors (e.g., the hydrolytic properties of the "clean" surface, surface clusters and isolated ions). Isolated, unhydrolyzed cations clearly make the greatest positive contribution to the electrophoretically measured charge, per ion adsorbed. Since clusters apparently form and exert a significant effect on the EM [cf. (16)], the surface to volume ratio of these clusters must be quite high.

ESR spectra similar to the ones in Fig. 7 have been reported by several workers for Mn(II) adsorbed on a variety of materials (15, 39, 41–44). The analysis of this type of spectrum has varied considerably. Perhaps the point at which to begin this discussion should be the relaxation processes that act on Mn(II) and their expression in the ESR spectra of this species.

The dominant anisotropic term in the spin Hamiltonian of Mn(II) in a high spin complex is the zero-field-splitting (ZFS) tensor (35–39). The ZFS tensor for a complex with cubic symmetry is identically zero. Zero-field splitting arises from the removal of spin level degeneracy by an asymmetric crystal field. The ZFS term does not contribute to the static part of the spin Hamiltonian, but through its contri-

bution to the time-dependent part of the Hamiltonian it becomes the major source of spin relaxation in an Mn(II) ESR experiment.

The formation of an asymmetric complex with a surface site will produce a nonzero ZFS term (15, 40–42). Such a complex could be "outer-sphere," leaving the first hydration sphere intact, and still yield a nonzero ZFS term (40).

If Mn(II) is strongly bound to a low symmetry site, the nonzero ZFS term would provide a pathway for spin relaxation through spin-lattice coupling. The hyperfine peaks would be broader while the g value and hyperfine splitting, which are sensitive to the crystal-field environment, would be different from those hexaquomanganese(2+). Alternatively, the Mn(II) could be weakly held in a low symmetry site and undergoing rapid tumbling. The broadening in this case would result from distortions of the inner-hydration sphere caused by the low symmetry site, equivalent to a fluctuating distortion model, but the g value and the hyperfine splitting should be the same as those for hexaquomanganese(2+) (44). We would expect narrowing in the latter case as the suspension is frozen since freezing would in effect form a "static" outersphere complex. A "static" outersphere complex would likely have a lower ZFS term than a rigidly held innersphere complex.

We propose that the Mn(II) species giving rise to the six, broadened hyperfine peaks (Figs. 7A and B) are freely tumbling in isolated, low symmetry sites with their inner-hydration sphere intact. The g value and hyperfine splitting constant are the same as those for hexaquomanganese(2+). It is quite possible that Mn(II) forms strong complexes with isolated surface sites which are undetectable by ESR. Roy *et al.* (15) found that only a small fraction of the total Mn(II) in the system (10% in their case) contributed to the ESR peak intensity.

Spin exchange is another factor which contributes to the ESR line broadening for Mn(II) adsorbed on surfaces (27, 39–43). This exchange broadening arises as the concentration of adsorbed Mn(II) increases and the average distance separating ions decreases. In many cases this exchange interaction is attributed solely to coupled paramagnetic species (27, 28, 43). Martini (39) reported a composite spectrum interpreted as arising from paramagnetic species subject to nonzero ZFS effects and Mn(II) salts formed in the pores of silica as the solution froze. The temperature-dependent peak intensity of the broad spectrum (Fig. 8) is indicative of a material that is antiferromagnetic. This could arise only from strongly exchange coupled spins as would exist in surface clusters. The broad ESR spectra observed at the highest Mn(II) level supports this conclusion.

We believe the ESR spectra of Figs. 7A–D and Fig. 8 consist of a paramagnetic signal superimposed on a symmetric peak due to Mn(II) in surface clusters. Based on the effect of Mn(II) adsorption on the suspension EM, we propose that much of the Mn(II) on the surface resides in surface clusters in which the effect of adsorbed ions on electrophoretically measured charge is minimized.

Between pH = 5.0 and pH = 5.1 some form of oxidized Mn appears on the surface of the titanium dioxide; however, the amount of Mn involved in this oxidation is a very small portion of the total Mn in the system. The factor limiting the extent of oxidation is not clear.

According to Coughlin and Matsui (45) the catalysis of Mn(II) oxidation in oxygen-containing titanium dioxide suspensions can be described by a model which combines adsorption of Mn(II) and molecular oxygen by the oxide surface. The reaction then occurs between the adsorbed species. However, titanium dioxide is a known photosemiconductor (46). Band-gap photo-excitation by 355-nm light creates electron-hole pairs which have a lifetime on the order of ms (47) and are capable of oxidizing water. Clearly an oxidizing agent this strong could oxidize adsorbed Mn(II). If this reaction were to proceed in the absence of oxygen dissolved in solution it would probably cease once the surface of the titanium dioxide became significantly reduced. While the oxidation we observe may be due to mo-

lecular oxygen adsorbed on the surface and not removed by our technique, this seems unlikely. We saw no oxidation of this sort when Mn(II) adsorbed on boehmite under precisely the same conditions (16). It is more likely that the oxidation is photo-induced and limited by the reduction of the surface in an oxygen-free system.

SUMMARY

Adsorption of Cu(II) on the surface of titanium dioxide begins at pH = 2 with the occupation of isolated sites having relatively high crystal fields. These sites hold Cu(II) in "static" tetragonal coordination. It appears that these sites, while few in number, are not uniformly distributed since broadening (presumably via spin-exchange coupling) occurs at very low surface coverage. The sharp increase in the surface excess concentration of Cu(II) and the appearance of a composite ESR spectrum at pH = 4.4 indicate the formation of hydrous-Cu(II) clusters on the surface of the titanium dioxide at that pH. This is further supported by the existence of paramagnetic Cu(II) on the surface when there is sufficient Cu(II) to form a complete monolayer of close-packed, hydrated ions. The evidence is clear that Cu(II) is not distributed uniformly on the surface, even at very low levels of adsorption.

Mn(II) begins adsorption below the IEP of titanium dioxide, but the ESR signal for solution species mask surface species until about pH = 5.5. As in the case for Cu(II), Mn(II) appears to adsorb by both occupying relatively isolated sites and forming surface clusters. A limited amount of the Mn(II) oxidizes rapidly upon adsorption under oxygen-free conditions, most likely a photo-induced oxidation by the titanium dioxide surface.

In conclusion, we feel the most significant result reported in this paper is that two distinct mechanisms for metal ion adsorption can coexist in aqueous oxide suspensions. While it may be suitable to model the discrete, metal-ion/site complex by analogy with coordination complexes formed in solution; surface-cluster formation cannot be described by such an analogy. Just as the activity products for precipitation phenomena differ from those for the formation of coordination complexes, so also should we expect the thermodynamic description of surface-cluster formation to differ from that appropriate for discrete, adsorbate/site complexes. We should consider the surface cluster as a site for adsorption, but a site that is not "filled" by being occupied. Rather, as we observed in an earlier paper (16), the very process of adsorption creates new adsorption sites that were nonexistent on the "clean" surface.

REFERENCES

1. Hachiya, K., Sasaki, M., Saruta, Y., Mikami, N., and Yasunaga, T., *J. Phys. Chem.* **88,** 23 (1984).
2. Westall, J., and Hohl, H., *Adv. Colloid Interface Sci.* **12,** 265 (1980).
3. Davis, J. A., and Leckie, J. O., *J. Colloid Interface Sci.* **67,** 90 (1978).
4. Motschi, H., *Naturwissenschaften.* **70,** 519 (1983).
5. Zelewsky, A. von, and Bemtgen, J.-M., *Inorg. Chem.* **21,** 1771 (1982).
6. Motschi, H., *Colloids Surf.* **9,** 333 (1984).
7. Richardson, J. T., *J. Catal.* **9,** 178 (1967).
8. Heitner-Wirguin, C., and Cohen, R., *J. Phys. Chem.* **71,** 2556 (1967).
9. Nicula, A., Stamires, D., and Turkevich, J., *J. Chem. Phys.* **42,** 3684 (1965).
10. Lumbeck, H., and Voitlander, J., *J. Catal.* **13,** 117 (1969).
11. Matsunaga, Y., *Bull. Chem. Soc. Japan* **34,** 1291 (1961).
12. Berger, P. A., and Roth, J. F., *J. Phys. Chem.* **71,** 4307 (1967).
13. Deen, R., Scheltus, P. I. Th., and de Vries, G., *J. Catal.* **41,** 218 (1976).
14. Bogdanov, V. A., Shveta, V. A., and Kazanskii, V. B., *Kinet. Catal. Engl. Transl.* **15,** 150 (1974).
15. Roy, R., Cogneau, M. A., Debuyst, R., and Apers, D. J., *Bull. Soc. Chim. Belg.* **82,** 75 (1972).
16. Bleam, W. F., and McBride, M. B., *J. Interface Sci.* **103,** 124 (1985).
17. McBride, M. B., *Clays Clay Miner.* **30,** 21 (1982).
18. Kavalerova, E. V., Golubev, V. B., and Evdokimov, V. B., *Russ. J. Phys. Chem.* **37,** 116 (1963).
19. Cozar, O., Znamirovschi, V., and Gridan, M., *Rev. Roum. Phys.* **27,** 289 (1982).
20. Tikhomirova, N. N., and Nikolaeva, I. V., *J. Struct. Chem. Engl. Transl.* **10,** 457 (1969).
21. Heimnetz, P. C., "Principles of Colloid and Surface Chemistry." Dekker, New York, 1977.

22. Attanasio, D., Collamati, I., and Ercolani, C., *J. Chem. Soc. Dalton Trans.* **12,** 1319 (1974).
23. Hronsky, V., and Rakos, M., *Czech. J. Phys. B* **33,** 1347 (1983).
24. Wertz, J. E., and Bolton, J. R., "Electron Spin Resonance: Elementary Theory and Practical Applications." McGraw–Hill, New York, 1972.
25. Abragam, A., and Bleaney, B., "Electron Paramagnetic Resonance of Transition Ions." Clarendon, Oxford, 1970.
26. Bleaney, B. I., and Bleaney, B., "Electricity and Magnetism." Oxford Univ. Press, Oxford, 1978.
27. Faber, R. J., and Rogers, M. T., *J. Amer. Chem. Soc.* **81,** 1849 (1959).
28. McBride, M. B., *Soil Soc. Soc. Amer. J.* **42,** 27 (1978).
29. Martini, G., Bassetti, V., and Ottaviani, M. F., *J. Chim. Phys.* **77,** 213 (1980).
30. Bassetti, V., Burlamacchi, L., and Martini, G., *J. Amer. Chem. Soc.* **101,** 5471 (1979).
31. Cozar, O., and Znamirovschi, V., *Czech. J. Phys. B* **33,** 1357 (1983).
32. Martini, G., and Ottaviani, F., *Z. Naturforsch.* **38,** 723 (1983).
33. Fujiwara, S., Katsumata, S., and Seki, T., *J. Phys. Chem.* **71,** 115 (1967).
34. Lyklema, J., *J. Colloid Interface Sci.* **99,** 109 (1984).
35. Burlamacchi, L., *J. Chem. Phys.* **55,** 1205 (1971).
36. Poupko, R., and Luz, Z., *Mol. Phys.* **36,** 733 (1978).
37. Burlamacchi, L., Martini, G., Ottaviani, M. F., and Romanelli, M., *Adv. Mol. Relax. Interact. Processes* **12,** 145 (1978).
38. Romanelli, M., and Burlamacchi, L., *Mol. Phys.* **31,** 115 (1976).
39. Martini, G., *J. Colloid Interface Sci.* **80,** 39 (1981).
40. Burlamacchi, L., Ottaviani, M. F., Ceresa, E. M., and Visca, M., *Colloids Surf.* **7,** 165 (1983).
41. Hronsky, V., Rakos, M., Belak, J., Juhar, J., and Kazar, D., *Czech. J. Phys. B* **28,** 1277 (1978).
42. Vishnevskaya, G. P., Safin, R. Sh., Ramazanov, R. G., and Gorozhanin, V. A., *Theor. Exp. Chem. Engl. Transl.* **16,** 492 (1980).
43. Hronsky, V., and Rakos, M., *Czech. J. Phys. B* **30,** 1061 (1980).
44. Burlamacchi, L., and Villa, P. L., *React. Kinet. Catal. Lett.* **3,** 199 (1975).
45. Coughlin, R. W., and Matsui, I., *J. Catal.* **41,** 108 (1976).
46. Rossetti, R., Beck, S. M., and Brus, L. E., *J. Amer. Chem. Soc.* **106,** 980 (1984).
47. Duonghong, D., Ramsden, J., and Gratzel, J., *J. Amer. Chem. Soc.* **104,** 2977 (1982).